A Synchronous Current Inversion and Energy Extraction Circuit for Electromagnetic Energy Harvesting

Jiacong Qiu and Junrui Liang
School of Information Science and Technology
ShanghaiTech University, Shanghai 201210, China
Email: {qiujc, liangjr}@shanghaitech.edu.cn

2024 IEEE International Symposium on Circuits and Systems (ISCAS) | 979-8-3503-3099-1/24/$31.00 ©2024 IEEE | DOI: 10.1109/ISCAS58744.2024.10558233

***Abstract*—Synchronous switch (SS) technique has been extensively studied in piezoelectric energy harvesting (PEH). The SS circuits can significantly enhance the output power under the same vibration excitation. Some SS solutions have also been developed for an inductive electromagnetic (EM) source by referring to its capacitive PEH counterpart and taking a complementary design. This paper proposes a synchronized current inversion and energy extraction (SCIEE) circuit for EM energy harvesting (EMEH). SCIEE utilizes two switched capacitive branches to carry out the synchronized current inversion at the electromotive voltage negative-to-positive zero-crossing instants and energy extraction at the voltage positive-to-negative zero-crossing instants. Theoretical analysis shows that the proposed circuit is suitable to be used with an EM transducer, whose quality factor is relatively large. Experiments show that, under the same mechanical excitation, SCIEE can harvest 25% more power compared with the cutting-edge synchronized switch energy extraction (SSEE) circuit for EMEH.**

***Index Terms*—Electromagnetic energy harvesting (EMEH), synchronous switch interface circuit**

I. Introduction

Energy harvesting (EH) technology has been extensively studied in the last two decades. It is developed to collect, convert, and utilize ambient energy, which is widely distributed in our surroundings. The energy in different physical forms can be converted into electricity by using suitable transducers and power conditioning circuits. The harvested energy can be used to power embedded devices and wireless sensing nodes. These devices have the potential to become self-powered to get rid of environmentally unfriendly chemical batteries. Moreover, EH technology helps relieve battery recharging or replacement; therefore, reducing the maintenance cost.

Piezoelectric transducers (PTs) have a simple structure and relatively high output voltage. It has been extensively utilized for kinetic energy harvesting. The output impedance of a PT is capacitive and has a relatively higher magnitude compared with an EM one. The harvested power can be significantly enhanced by using the synchronized switch (SS) circuits. For example, by using the synchronous electric charge extraction (SECE) [1], one of the most studied SS circuits, the harvested power can be increased to 400% of that optimistically harvested by a full-wave bridge rectifier (FBR). Later, more harvesting circuits based on the synchronized switch principle have been proposed [2], [3], [4].

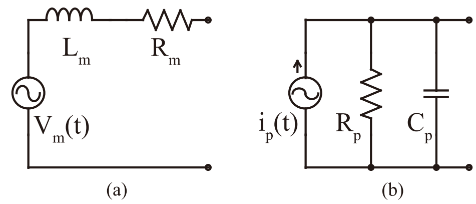

Fig. 1. Equivalent circuits of electromagnetic and piezoelectric transducers under constant velocity magnitude vibration excitation. (a) Electromagnetic. (b) Piezoelectric.

On the other hand, an electromagnetic (EM) transducer is the most widely used type of electromechanical transducer. It has higher power density and lower output impedance. However, the output voltage in the EM transducer is usually relatively much lower, compared with the PT case. Fig. 1 shows the equivalent circuit model of the EM and PT transducers. In the EM case, L_m and R_m are the equivalent series inductance (ESL) and equivalent series resistance (ESR) of the coil winding. In the PT case, C_p and R_p are the piezoelectric capacitance and parasitic dielectric leakage resistance of a PT. Their equivalent circuits are symmetrical, in terms of a voltage source with inductive source impedance versus a current source with capacitive source impedance. Considering the complementary relation, those SS solutions for PEH enhancement by manipulating the voltage by referring to the current phase might correspond to some SS solutions that manipulate the current by referring to the voltage phase in the EM case.

Some studies have validated the performance of SS for EM transducers. Ref. [5] proposed an SECE-symmetric design for EM transducers and named this method synchronous magnetic flux extraction (SMFE). Ref. [6] proposed an improved and self-powered version named synchronous switch energy extraction (SSEE). The measured harvested power is nearly twice of the maximum output power of FBR under the same mechanical excitation. The authors also explored the applications of SS for regenerative motor brake [7]. Some studies [3], [8] combined the synchronous voltage inversion and charge extraction in an interleaving way to further enhance the harvested power. This paper studies its counterpart for the

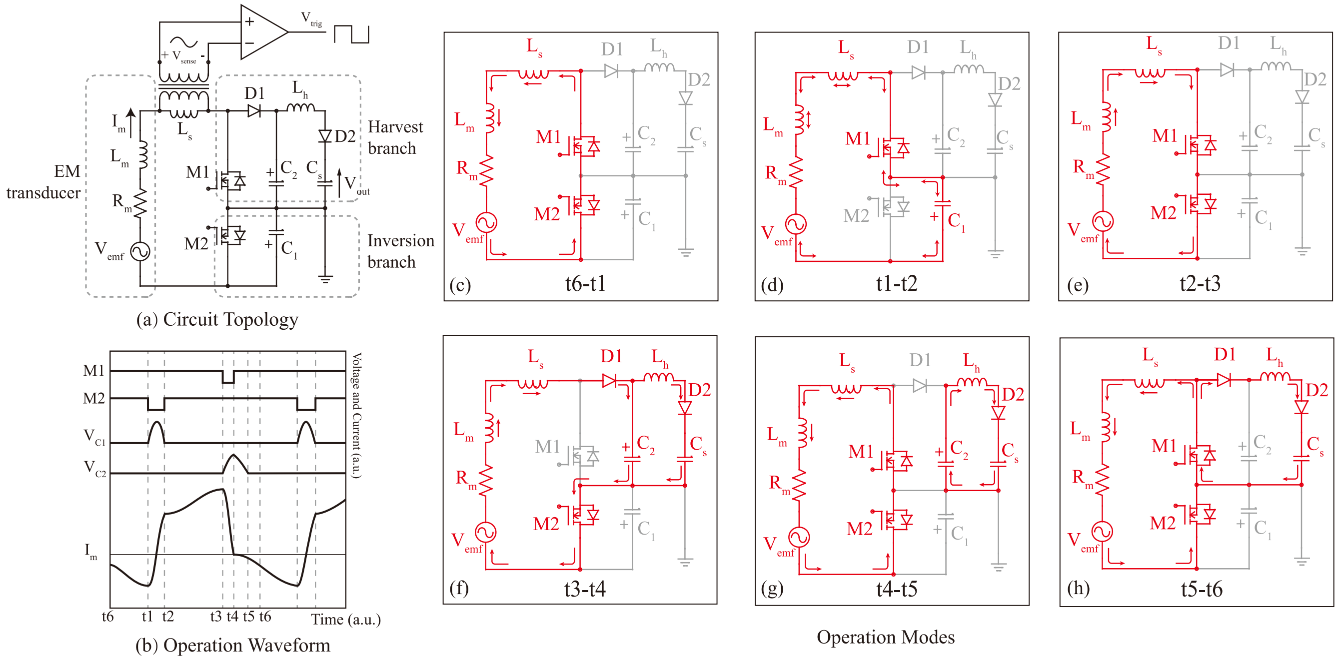

Fig. 2. Circuit topology, operation waveform, and operation modes of SCIEE circuit.

EM transducers. We proposed a circuit called synchronized current inversion and energy extraction (SCIEE) for EMEH enhancement.

II. Proposed SCIEE Circuit

Fig. 2 shows the proposed circuit topology, where V_{emf}, R_m, and L_m are the equivalent electromotive voltage, ESR, and inductance of the EM transducer. C_s is the output filter capacitor supporting the dc load. M_1, D_1, and C_2 forms the harvesting (energy extraction) branch, while M_2 and C_1 forms the current inversion branch.

The synchronous actions take place at the current extreme instants; therefore, finding the current peaks is crucial for proper circuit operation. In this study, the synchronization is realized by connecting a series sensing inductor L_s. The inductance L_s is much smaller than L_m; therefore, the divided voltage across L_s is negligible compared to that across L_m. The quality factor of L_s is designed to be the same as L_m, making the zero crossing point (ZCP) of voltage across L_s and R_s follows a peak of the source current. To measure this voltage, a 1:1 transformer is connected across L_s. The output voltage V_{sense} is fed to a comparator for ZCP detection. The rising edge and falling edge of comparator output V_{trig} indicate the current peak instants of the EM transducer.

A. Operation Principle

As shown in Fig. 2(c), from instants t6 to t1, both M_1 and M_2 conduct, the EM transducer is short-circuited, V_{emf} magnitizes L_m. Energy accumulates inside the transducer coil. This mode lasts until I_m reaches its peak.

At the t1 instants, when I_m reaches its negative peaks, M_2 is turned off; therefore, the current that originally flows through M_2 freewheels through the C_1 path. L_m and C_1 form an LC resonant loop. The time interval between t1 and t2 instants is controlled to a half LC resonant period. The I_m direction inverts from negative to positive during this period. Given that current induces torque to a rotational machine and force to a translational energy harvester, the current inversion introduces an in-phase torque/force to the angular velocity/translational velocity, which hinders the movement. In other words, extract more energy from the rotational or vibrational movement [9] throughout a whole cycle. At t2 instant, M_2 conducts again as V_{C1} returns zero.

After the t2 instant, the EM transducer is again short-circuited by M_1 and M_2, and energy accumulates inside the coil inductance L_m. This mode lasts until I_m reaches its positive peak at the t3 instant.

At the t3 instant, I_m is at the positive peak. We turn off M_1 to redirect I_m to the harvesting branch through diode D_1. The conduction of the harvesting branch consists of two stages. D_1 and C_2 form the first-stage shunt circuit. During this stage, L_m and C_2 form an LC resonant loop. Since the harvesting inductance L_h is designed much larger than transducer inductance L_m, when L_m and C_2 resonate, there is almost no current flowing through L_h. The sensing inductance $L_s \ll L_m$, so L_s also has little impact. After a quarter resonant period, I_m drops to zero. Most energy stored in the source inductance L_m is extracted and transferred to C_2. Only a small portion is transferred to L_h and C_s, given a relatively large L_h. This two-stage energy extraction and transferring design ensures fast energy extraction and stable storage [7].

After the t4 instant, M_1 conducts again. The EM transducer is short-circuited and starts accumulating energy by magnetizing L_m with negative V_{emf} in the other half cycle. D_1 is

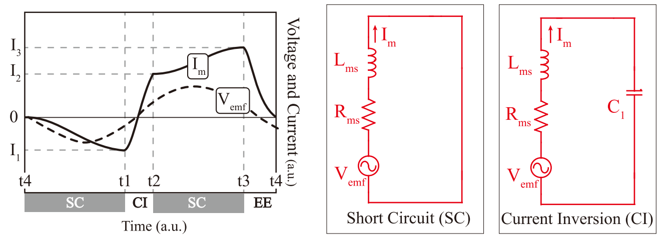

Fig. 3. Operation waveform of EM transducer current and simplified equivalent circuit during short circuit and current inversion.

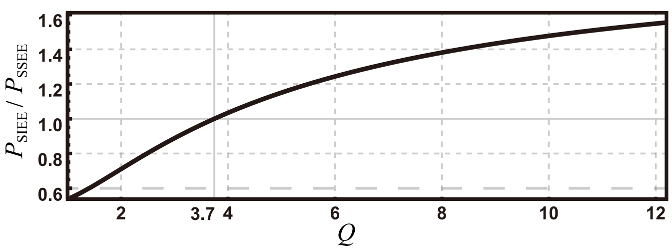

Fig. 4. Ratio of theoretical harvested powers in SCIEE and SSEE (given $Q_e = 10Q$).

reverse biased. C_2 and L_h forms a resonant loop. C_s is the output filter capacitor. It is designed to be large; therefore, can be considered a constant voltage source. The transient LC resonance proceeds until C_2 is fully discharged at t5 instant. During this phase, the energy stored in C_2 freewheels through L_h and is transferred to the storage filter capacitor C_s.

After the t5 instant, C_2 is completely discharged. But the current through L_h is still not zero. D_1 is forward-biased automatically again. The energy stored in L_h further freewheels through D_2 and C_s. This mode lasts until the current through L_h drops to zero at t6 instant. After that, i.e., the t6 instant, D_1 and D_2 are reverse biased. The source inductance L_m continues the magnetization in a short-circuit state.

III. Theoretical Analysis

As the previous section has introduced, the energy in the EM transducer is extracted to the harvesting branch between the t3 to t4 instants. In this phase, all energy stored in the inductance L_m is depleted and most is transferred to C_s eventually.

Fig. 3 shows the EM transducer's current waveform, which corresponds to the operation waveform shown in Fig. 2 (b). The current inversion (CI) phase has been stretched and emphasized to facilitate more detailed observation. First, we assume the electromotive force (generated voltage) is a sinusoidal voltage

$$V_{emf} = -V_0 \sin(\omega t), \tag{1}$$

where ω is the vibration angular frequency; V_0 is the magnitude. In the short-circuit (SC) phase, the inductance L_m and L_s are magnetized for half a resonance period. The current I_m can be formulated with a first-order differential equation

$$V_{emf}(t) = L_{\text{ms}} \frac{\mathrm{d}I_m(t)}{\mathrm{d}t} + R_{\text{ms}} I_m(t), \tag{2}$$

where $L_{\text{ms}} = L_m + L_s$; $R_{\text{ms}} = R_m + R_s$. Given zero initial current at the t4 instant, i.e., $I_m(0) = 0$, by solving (2) we have the current value at t1 instant

$$I_m(t1) = I_1 = V_0 \left(1 + e^{-\frac{\pi R_{\text{ms}}}{\omega L_{\text{ms}}}}\right) \frac{\omega L_{\text{ms}}}{R_{\text{ms}}^2 + \omega^2 L_{\text{ms}}^2}. \tag{3}$$

In the CI phase (t4 to t1), an RLC resonant circuit resonates for half a resonance period to inverse the current through the transducer coil. The end current I_2 is formulated by multiplying an inversion factor γ, like that in the PEH SS case, i.e.,

$$I_2 = \gamma I_1, \tag{4}$$

where

$$\gamma = -e^{-\frac{\pi}{2Q_e}}. \tag{5}$$

$Q_e = \omega_e L_{\text{ms}}/R_{\text{ms}}$ is the quality factor during current inversion; $\omega_e = (L_{\text{ms}} C_1)^{-1/2}$ is the resonant frequency of the L_{ms} and C_1 circuit.

In the other half-cycle SC phase, the circuit equation is the same as (2). But the initial condition changes from zero current to I_2. The integral interval approximately changes to $[t2, t3]$. The final current I_3 is obtained as follows

$$I_3 = I_1 + |I_2| e^{-\frac{\pi}{Q}}, \tag{6}$$

where $Q = \omega L_{\text{ms}}/R_{\text{ms}}$ is the transducer's mechanical quality factor.

Since all energy accumulated in one cycle in the EM transducer coil is released at the $t3$ instant, the total extraction energy in one cycle by an SCIEE circuit is formulated by

$$E_{\text{SCIEE}} = \frac{1}{2} L_m I_3^2. \tag{7}$$

On the other hand, in SSEE [6], the EM transducer energy output in one cycle was formulated by [6]

$$E_{\text{SSEE}} = L_m I_1^2. \tag{8}$$

By substituting (3), (4), and (6) into (7) and (8), the harvested energy in each vibration cycle and their ratio can be calculated. When mechanical excitation is the same, both harvesting circuits operate under the same frequency f. The harvested power can be obtained by multiplying the harvested energy with the harvested frequency f. The ratio of harvested power between SCIEE and SSEE can be calculated as follows

$$\frac{P_{\text{SCIEE}}}{P_{\text{SSEE}}} = \frac{f E_{\text{SCIEE}}}{f E_{\text{SSEE}}} = \frac{\left[e^{-\left(\frac{\pi}{Q} + \frac{\pi}{2Q_e}\right)} + 1\right]^2}{2}, \tag{9}$$

According to (9), Fig. 4 shows the power ratio between SCIEE and SSEE in some Q range. It shows that SSEE gives larger harvested power when the quality factor Q is relatively low, approximately under four. But as Q increases, P_{SCIEE} increases faster than P_{SSEE}. when $Q > 3.7$, the harvested power of SCIEE outperforms that of SSEE. Therefore, we can summarize that the proposed circuit is more suitable for EM transducers possessing a relatively large quality factor.

TABLE I
COMPONENT PARAMETERS IN EXPERIMENT.

Component	Value / Type
Resonance capacitors C_1,C_2	2 μF
Output capacitor C_s	33 μF
Transducer internal inductance L_m	1.2 mH (ESR = 0.20 Ω)
Transducer frequency f	333 Hz
Transducer voltage amplitude V_0	1.15 V
Transducer quality factor Q	12.35 @ 333 Hz
Quality factor of resonant circuit Q_e	123.5 @ 3330 Hz
Harvesting inductors L_h	12.0 mH (ESR = 0.9 Ω)
Sensing inductor L_s	0.2 mH (ESR = 35 mΩ)
N-channel MOSFET	IPT015N10N5 ($R_{\mathrm{DS(on)}}$ = 1.5 mΩ)
Diodes	1N4004 (400 V, 1 A)
Comparator	LMC7211BIM5
1:1 transformer	UU9.8Y - 10 mH

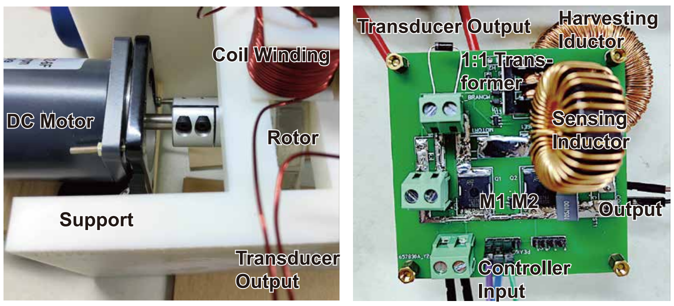

Fig. 5. Experimental setup.

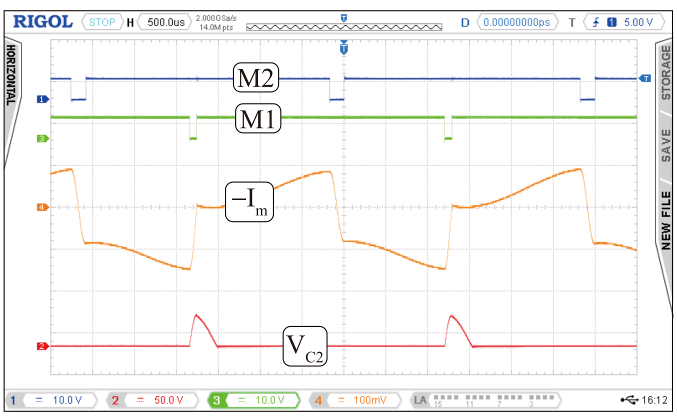

Fig. 6. Measured waveform.

IV. EXPERIMENTS

A. Setup

A printed circuit board (PCB) prototype is fabricated to validate the proposed design. By changing some components, the prototype can switch between SCIEE and SSEE modes. Both modes share the same switches and inductors for fair comparison. The components used in experiments and their values are listed in Table I.

Fig. 5 shows the EM transducer and PCB prototype used in the experiment. The EM transducer is driven by a dc motor. The open-circuit output voltage of the EM transducer is a sinusoidal wave, whose peak-to-peak value is 3.3 V and frequency is 333 Hz. The switched-mode circuit is driven by an externally powered microcontroller in this design. According to a rough guess, when the two IPT015N10N5 MOSFETs (gate capacitance 12 nF) are driven at 333 Hz, the required power is calculated to be around 1 mW. So with careful design and a low-power microcontroller, the self-powered issue is achievable in our future design [6]. This paper investigates the working principle first. The self-powering issue will be considered in future work.

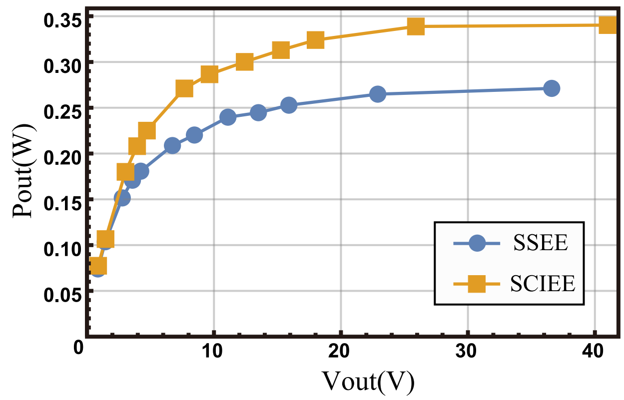

Fig. 7. Harvested power in experiment.

Fig. 6 shows the steady-state operation waveform when the output voltage $V_{out} = 9$ V. The third curve in orange is the transducer current measured by a current probe (1 A corresponds to 0.1 V in measurement). The fourth curve in red is the voltage across C_2. The experimental waveform agrees with the conceptual designed one, which was shown in Fig. 2, quite well. The experimentally measured $I_{1\mathrm{exp}} = 0.8$ A and $I_{3\mathrm{exp}} = 1.4$ A. Substituting $I_{1\mathrm{exp}}$ and $I_{3\mathrm{exp}}$ back to (6) yields $Q = 11.45$, which is close to experimentally measured value 12.2. The error might be caused by other ESRs in C_1 and circuit connections. This validates the theoretical analysis.

The harvested power by using the proposed SCIEE circuit is measured and compared with that using SSEE under the same mechanical excitation. Fig. 7 shows the measured harvested power under different output voltages, which can be varied by changing the load resistance. Experiments show that SCIEE harvests more power than SSEE under all loading conditions. As the output voltage gets larger, the percentage of power enhancement approaches 25%.

V. CONCLUSION

This article proposed a synchronous current inversion and energy extraction (SCIEE) circuit for electromagnetic (EM) energy harvesting. Theoretical analysis suggested that SCIEE can extract more energy from an EM transducer possessing a quality factor above 3.7. A PCB circuit prototype was fabricated to evaluate the circuit's operation and performance. Compared with the synchronized switch energy extraction (SSEE) scheme, SCIEE can harvest 25% more power in experiments.

References

[1] E. Lefeuvre, A. Badel, C. Richard, and D. Guyomar, "Piezoelectric energy harvesting device optimization by synchronous charge extraction," *Journal of Intelligent Material Systems and Structures*, vol. 16, pp. 865–876, 10 2005.

[2] E. Lefeuvre, A. Badel, C. Richard, L. Petit, and D. Guyomar, "A comparison between several vibration-powered piezoelectric generators for standalone systems," *Sensors and Actuators A: Physical*, vol. 126, no. 2, pp. 405–416, 2006.

[3] M. Lallart, W.-J. Wu, Y. Hsieh, and L. Yan, "Synchronous inversion and charge extraction (sice): a hybrid switching interface for efficient vibrational energy harvesting," *Smart Materials and Structures*, vol. 26, no. 11, p. 115012, 2017.

[4] B. Ciftci, S. Chamanian, H. Ulusan, H. A. Yigit, A. Koyuncuoglu, A. Muhtaroglu, and H. Kulah, "Low-cost fully autonomous piezoelectric energy harvesting interface circuit with up to 6.14x power capacity gain," in *2019 IEEE Custom Integrated Circuits Conference (CICC)*, 2019, pp. 1–4.

[5] E. Arroyo and A. Badel, "Electromagnetic vibration energy harvesting device optimization by synchronous energy extraction," *Sensors and Actuators A: Physical*, vol. 171, no. 2, pp. 266–273, 2011.

[6] Z. Xie, L. Teng, H. Wang, Y. Liu, M. Fu, and J. Liang, "A self-powered synchronous switch energy extraction circuit for electromagnetic energy harvesting enhancement," *IEEE Transactions on Power Electronics*, vol. 38, no. 8, pp. 9972–9982, 2023.

[7] Z. Xie, L. Teng, Y. Yin, and J. Liang, "Synchronous switch energy extraction circuit for motor regenerative braking enhancement," *IEEE Transactions on Circuits and Systems II: Express Briefs*, vol. 70, no. 5, pp. 1779–1783, 2023.

[8] C.-W. Chen, W. Z. Pranoto, H.-S. Chen, and W.-J. Wu, "A 0.25-μm hv-cmos synchronous inversion and charge extraction interface circuit with a single inductor for piezoelectric energy harvesting," *IEEE Transactions on Power Electronics*, 2023.

[9] L. Teng, Z. Xie, Y. Yu, and J. Liang, "Synchronous switch current reversion (sscr) technique for motor braking enhancement," in *2022 IEEE Energy Conversion Congress and Exposition (ECCE)*, 2022, pp. 1–5.